INTERNATIONAL JOURNAL OF
COASTAL & OFFSHORE ENGINEERING
IJCOE Vol.2/No. 1/Spring 2018 (59-66)

Available online at: http://ijcoe.org/browse.php?a_code=A-10-61-1&sid=1&slc_lang=en

Free Vibration Analysis of Very Large Rectangular Floating Structures

Tannaz Hadizade Asar[1], Keyvan Sadeghi[2*], Arefeh Emami[3]

[1] *MSc graduate, Faculty of Civil Engineering, University of Hormozgan; tannaz.1365@yahoo.com*
[2*] *Corresponding author: Assist. Prof., Buein Zahra Technical University, Qazvin, Iran; keyvan.sadeghi@bzte.ac.ir*
[3] *PhD candidate, Faculty of Civil Engineering, Sahand University of Technology, Tabriz, Iran; a_emami@sut.ac.ir*

ARTICLE INFO

Article History:
Received: 29 Apr. 2018
Accepted: 9 Jun. 2018

Keywords:
Very large floating structure
Mindlin theory
Hydroelastic behavior
Finite element method

ABSTRACT

The dynamic behavior of a very large rectangular floating structure is considered. The structure is modelled as a plate with free edges. Two different thicknesses are considered for the model. The Mindlin plate theory is used to formulate the structure behavior. Natural frequencies, mode shapes, and stress resultants of the structure are predicted by using finite element method. For this purpose, a MATLAB code is written. The same analysis is performed by using the ANSYS software. The results of these two analysis are compared with each other and with the available results in the literature, where close agreement is observed. Therefore, the written finite element code is found to be acceptable for prediction of the dynamic behavior of very large rectangular floating structures in early stages of design.

1. Introduction

A very large floating structure (VLFS) is a viable alternative for land reclamation from coastal waters. VLFSs have been constructed as floating bridges, airports/heliports, oil storage systems, emergency rescue bases, industry spaces, hotels and amusement facilities. Compared to the traditional land reclamation methods, VLFSs are environmentally friendly, easy to construct and to remove or expand, less susceptible to earthquakes and cost effective, especially in deep coastal waters.

There are two major types of VLFS; namely the pontoon type and the semi-submersible type. The pontoon type has high stability, low manufacturing cost and is easy to repair. However, this type of VLFS is only suitable for calm waters in naturally sheltered areas or where breakwaters are constructed nearby [1]. The structure of a typical pontoon-type VLFS features a small depth to length ratio so it can be considered as a thin flat structure. In the horizontal plane, and for the design of the mooring system, the structure can be assumed to be rigid, however, in the vertical plane the elastic behavior of the thin structure cannot be ignored. A hydroelastic response analysis is, therefore, necessary. In this regard, the entire structure of a pontoon-type VLFS is usually modelled as a two-dimensional floating elastic plate with free edges [2]. For the hydroelastic analysis, different plate theories can be employed. The classical thin plate theory and the first-order shear deformation (Mindlin) plate theory are commonly used. For a VLFS the fluid-structure interaction problem includes the elastic deformations as well as the rigid body motions

In literature, there are many studies regarding to VLFS dynamical behavior where a variety of analytical and numerical methods have been used. Liew and Hun [3] investigated the dynamic behavior of a rectangular plate using the approximate least squares method. They considered the effect of shear deformation, flexural and torsional moments and shear forces using Winkler assumption and Mindlin plate theory. Xiang [4] studied the eigenvalues of vibrating plates using the first-order shear deformation theory. Rossi and Bambill [5] evaluated analytically the transverse vibrations and natural frequencies of a homogeneous rectangular plate with four different boundary conditions. Wang et al [6] showed that the Ritz and finite element methods do not satisfy natural boundary conditions in stress resultants of shear force and twisting moments at plate free edges. Beirao da Veiga [7] presented an extension of different families of well-known optimal plate models based on a modified free boundary model for plates with free edges. The hydroelastic analysis of a pontoon-type VLFS was studied by Wang et al. [8]. They studied the wave forces, drift forces, the geometrical shape and the mooring system of a VLFS. To overcome the difficulties reported in [6] they used the least squares finite difference (LSFD) method. They showed that the LSFD method is better than the Ritz and Galerkin methods for prediction of stress resultants for plates with free edges. Wu et al [9] used the LSFD method based on the classical plate theory for prediction of

natural frequencies, mode shapes, and stress resultants of freely vibrating plates with circular, elliptic and triangular shapes. Ma and Ang [10] used a finite element formulation based on the Mindlin plate theory in terms of a relative displacement concept and an assumed strain method and find results that agree with theoretical solutions. Sadrnejad and Saedi Daryan [11] investigated the vibration of a thick rectangular plate using the first order shear deformation theory. They calculated the natural frequencies of a thick plate with different boundary conditions and discussed the effect of plate thickness and dimensions on its oscillatory behavior. Xiang et al [12] proposed a discrete singular convolution (DSC) method for the free vibration of moderately thick plates based on the first-order shear deformation theory. Xiang et al [13] applied DSC-Ritz element method for the vibration of rectangular plates with mixed edge supports using the same plate theory. Hosseini-Hashemi et al. [14] analytically investigated the free vibrations of moderately thick rectangular plates with different boundary conditions. Hosseini-Hashemi et al. [15] proposed an exact solution for free vibrations of Levy-type rectangular thick plates using the third-order shear deformation plate theory. Another study regarding a new exact analytical solution for free vibrations of Reissner-Mindlin functionally graded rectangular plates is reported by Hosseini-Hashemi et al. [16]. Ramu and Mohanty [17] studied the free vibrations of rectangular plate structures using finite element method. Pereira et al. [18] addressed a dynamic formulation for thick elastic plates using the boundary element method. Eftekhari and Jafari [19] used a modified mixed Ritz-differential quadrature formulation in which all natural boundary conditions were exactly implemented. Cho et al. [20] proposed a procedure based on the assumed mode method for vibration analysis of rectangular plates with openings and arbitrary edge constraints. Thai and Choi [21] analytically studied the bending, buckling, and vibration analysis of thick rectangular plates with various boundary conditions by a refined plate theory. Senjanovic et al [22] modified the Mindlin plate theory and proposed a shear locking-free finite element formulation. Praveen et al. [23] analyzed the hydroelastic behavior of floating elastic thick plates in shallow water depth. They investigated the effect of various boundary conditions. The vibrations of moderately thick plates were studied by Senjanovic et al. [24] based on the modified Mindlin theory using a dynamic finite element technique. Khezri et al. [25] studied thin to moderately thick plates based on the shear locking-free Mindlin theory formulation using a meshless analysis. Shirkol and Nasar [26] carried out a coupled boundary element-finite element method for analyzing the hydroelastic behavior of floating plates.

For preliminary design purposes an analytical/semi-analytical approach can be employed for hydroelastic analysis of vertical motions. In this simplified model the entire pontoon-type VLFS can be modelled as a two-dimensional floating plate with free edges. In a linear theory the hydroelastic response of the floating plate (the wet plate) can be obtained by the so-called dry mode superposition method [2], where the unknown flexural response of the wet plate is assumed as a linear combination of the mode shapes of an elastic plate in air (the dry plate). Once the unknown coefficients of the superposition response, i.e., the modal amplitudes are obtained, the stress resultants of the VLFS can be predicted.

In the modal method, the classical thin plate theory or the first-order shear deformation theory are commonly employed. In the latter theory, the transverse shear deformation and the rotary inertia are allowed. In addition, the stress resultants are related to first order derivatives of the deflections and rotations while in the classical thin plate theory third order derivatives of those functions are required to compute the stress resultants. That is why more accurate stress resultants can be obtained from the Mindlin plate theory compared to the classical thin plate theory.

The natural frequencies of the wet plate are lower than the corresponding values of the dry plate. This is because of the higher effective mass due to the added mass associated with the kinetic energy transferred to the heavy fluid. However, the mode shapes of the wet and dry plates are usually assumed to be virtually the same. It is well known that the finite element method (FEM) predicts the natural frequencies and the mode shapes of plates with free edges with excellent accuracy, however, the FEM results for stress resultants, especially for the transverse shear forces and the twisting moments are not satisfactory for plates with free edges. This is partly due to the presence of very steep gradients in the stress resultant distributions near the free edges and partly due to the fact that in a FEM solution, the natural boundary conditions are imposed in a weak form [8].

For correct prediction of hydroelastic behavior of VLFS structures, it is vital to obtain accurate natural frequencies, mode shapes and stress resultants of plates with free edges. In this paper, the natural frequencies, mode shapes and stress resultants of dry plates are derived by using the finite element method based on the first-order shear deformation plate theory. In this regard, a computer code is written in MATLAB. In addition the same problem is analyzed using the ANSYS software. The results of the MATLAB code and those of ANSYS are compared with each other as well as with the relevant LSFD results [8] and the accuracy of the written code is verified. It is shown that the written code can be used to predict the hydroelastic behavior of the pontoon-type VLFS in early stages of design.

2. Problem definition

Consider an isotropic, elastic, rectangular plate with length a and width b. The origin of the Cartesian

coordinate system is placed at the plate center in its mid-plane. The xy plane coincide with the plate mid-plane and the *z*-axis is vertically upwards. According to the first-order shear deformation theory, the differential equations of motion are as follows:

$$k\frac{1-\nu}{2}\left(w_{,xx}+w_{,yy}+\psi_{x,x}+\psi_{y,y}\right)=\frac{\rho h^3}{12D}w_{,tt} \tag{1}$$

$$\psi_{x,xx}+\frac{1-\nu}{2}\psi_{x,yy}+\frac{1+\nu}{2}\psi_{y,xy}-\frac{6k(1-\upsilon)}{h^2}\left(w_{,x}+\psi_x\right)=\frac{\rho h^3}{12D}\psi_{x,tt} \tag{2}$$

$$\psi_{y,yy}+\frac{1-\nu}{2}\psi_{y,xx}+\frac{1+\nu}{2}\psi_{x,xy}-\frac{6k(1-\upsilon)}{h^2}\left(w_{,y}+\psi_y\right)=\frac{\rho h^3}{12D}\psi_{y,tt} \tag{3}$$

where, w, ψ_x and ψ_y are the generalized displacement functions associated with an arbitrary point on the plate's mid-plane. They are the displacement in the vertical direction and rotations about x and y axes, respectively. In Eqs. (1) to (3) the comma notation is used to denote the partial differentiation. The parameters k, h and ν are the shear coefficient, the plate thickness and Poisson's ratio, respectively, and D is the flexural rigidity:

$$D=\frac{Eh^3}{12(1-\nu^2)}$$

where E is Young's modulus. The following equations relate the stress resultants to the generalized displacement functions:

$$M_{xx}=D\left(\psi_{x,x}+\nu\psi_{y,y}\right) \tag{4}$$

$$M_{yy}=D\left(\nu\psi_{x,x}+\psi_{y,y}\right) \tag{5}$$

$$M_{xy}=M_{yx}=D\frac{1-\nu}{2}\left(\psi_{x,y}+\psi_{y,x}\right) \tag{6}$$

$$Q_x=k\frac{Eh}{2(1+\nu)}\left(w_{,x}+\psi_x\right) \tag{7}$$

$$Q_y=k\frac{Eh}{2(1+\nu)}\left(w_{,y}+\psi_y\right) \tag{8}$$

The first two equations are for bending moments and the last two equations are for shear forces. The middle equation represnts the twisting moments. The boundary conditions at free edges are given by the following relation:

$$Q_x=Q_y=M_{xx}=M_{yy}=M_{xy}=0 \tag{9}$$

2.1. Free Vibrations of rectangular plate

The free vibrations are studied in the absence of external loads such as waves, winds and currents. If the continuous plate is approximated by a discrete system such as a finite element mesh, the equation of undamped free vibrations can be written as

$$[M]\{\ddot{x}\}+[K]\{x\}=0 \tag{10}$$

where $[M]$ and $[K]$ are the mass and stiffness matrices and $\{x\}$ is the vector of nodal displacements. Each node has three degrees of freedom, which are w, ψ_x and ψ_y. Therefore, if the number of nodes in the mesh is N the vector $\{x\}$ will be a $3N\times 1$ vector. Assuming harmonic displacements, Eq. (10) can be rewritten as

$$([K]-\omega_i^2[M])\{\hat{x}\}_i=0 \tag{11}$$

where $\{\hat{x}\}_i$ is the vector of nodal amplitudes or the i^{th} mode shape and ω_i is the i^{th} natural frequency.

2.2. Numerical Formulation

Each node in the finite element mesh is assumed to have three degrees of freedom, i.e., w_i, ψ_{x_i} and ψ_{y_i}. Therefore, the stiffness and mass sub-matrices associated with the i^{th} and j^{th} nodes of an element will be 3×3 symmetric matrices as follows

$$[K]_{ij}=\begin{bmatrix}K_{ij}^{11} & K_{ij}^{12} & K_{ij}^{13}\\ K_{ij}^{21} & K_{ij}^{22} & K_{ij}^{23}\\ K_{ij}^{31} & K_{ij}^{32} & K_{ij}^{33}\end{bmatrix}$$
$$[M]_{ij}=\begin{bmatrix}M_{ij}^{11} & 0 & 0\\ 0 & M_{ij}^{22} & 0\\ 0 & 0 & M_{ij}^{33}\end{bmatrix} \tag{12}$$

The generalized displacement functions are approximated as interpolations between nodal values, that is

$$\begin{aligned}w&=\textstyle\sum_{j=1}^{n}w_j\varphi_j\\ \psi_x&=\textstyle\sum_{j=1}^{n}\psi_{x_j}\varphi_j\\ \psi_y&=\textstyle\sum_{j=1}^{n}\psi_{y_j}\varphi_j\end{aligned} \tag{13}$$

where n is the number of nodes per element, and φ_j is the interpolation function of the j^{th} node of the element. Introducing from Eq. (13) into motion Eqs. (1) to (3), integrating over the element area and using the integration by parts technique, the weak form of the governing equations can be derived. Then, following the common procedure in the finite element method, the elements of the stiffness and mass sub-matrices can be obtained from the following relations:

$$K_{ij}^{11}=kGh\iint\left(\varphi_{,x_i}\varphi_{,x_j}+\varphi_{,y_i}\varphi_{,y_j}\right)dxdy$$

$$K_{ij}^{12} = kGh \iint \varphi_{,x_i} \varphi_j dxdy$$
$$K_{ij}^{13} = kGh \iint \varphi_{,y_i} \varphi_j dxdy$$
$$K_{ij}^{22} = \iint \left(D\varphi_{,x_i}\varphi_{,x_j} + \frac{Gh^3}{12}\varphi_{,y_i}\varphi_{,y_j} + kGh\varphi_i\varphi_j \right) dxdy$$
$$K_{ij}^{23} = \iint \left(\nu D\varphi_{,x_i}\varphi_{,y_j} + \frac{Gh^3}{12}\varphi_{,y_i}\varphi_{,x_j} \right) dxdy$$
$$K_{ij}^{33} = \iint \left(\frac{Gh^3}{12}\varphi_{,x_i}\varphi_{,x_j} + D\varphi_{,y_i}\varphi_{,y_j} + kGh\varphi_i\varphi_j \right) dxdy \quad (17)$$

and

$$M_{ij}^{11} = \rho h \iint \varphi_i \varphi_j dxdy$$
$$M_{ij}^{22} = M_{ij}^{33} = \frac{\rho h^3}{12} \iint \varphi_i \varphi_j dxdy \quad (18)$$

where in Eqs. (17) and (18) integrations are over the element area. The rectangular plate is discretized by 20×7=140 elements. Each element in the mesh is an eight-node rectangular serendipity element with quadratic interpolation functions.

2.3. Modeling by Ansys Software

ANSYS is a powerful finite element software that is widely used for solving various engineering problems including dynamic analysis of structures. In this paper, in addition to a MATLAB code, the ANSYS software is employed for the dynamic response analysis of a plate with free edges. For this purpose the Shell 93 element is used. Each node in this element, in general, has six degrees of freedom: three displacements in *x*, *y* and *z* directions and three rotations about the same axes. The displacement in the *x* and *y* directions and the rotation about the *z*-axis are fixed to reduce the number of degrees of freedom per node to 3. The dynamic analysis is carried out by using the modal module of ANSYS and the results are presented in the following sections.

3. Results and discussion

A rectangular plate with 4 m length, 1 m width, and a thickness of 0.1 m is analyzed by both the MATLAB code and the ANSYS software. Young's modulus, Poisson's ratio and the mass density are assumed to be 210 GPa, 0.3 and 7830 kg/m^3, respectively. The results of two numerical methods are compared with each other as well as with those of Wang et al [8], which are obtained from a least squares finite difference (LSFD) method.

3.1. Natural frequencies and mode shapes

Disregarding the rigid body modes, the frequency parameters for the first four mode shapes are reported in the following table. The dimensionless frequency parameter is defined as follows:

$$\Omega = \omega b^2 \sqrt{\frac{\rho h}{D}} = \frac{\omega b^2}{h} \sqrt{\frac{12\rho(1-\nu^2)}{E}} \quad (19)$$

In this table, the FEM (MATLAB and ANSYS) and LSFD results [8] are presented. As can be seen, they are in good agreement. The maximum values of the dimensionless generalized displacement functions corresponding to the first four mode shapes are given in Table 2. Figs 1-12 show the 1st to 4th mode shapes obtained from the MATLAB, ANSYS, and LSFD methods. As can be seen, the mode shapes are in close agreement. This confirms the findings of the previous research that the finite element method is very accurate in calculating natural frequencies and mode shapes of plates with free edges. However, mode shapes derived from the written code are not as accurate as those obtained from ANSYS. This can be due to using a rather coarse mesh in MATLAB and also due to the shear locking phenomenon.

Table 1. Frequency parameters of the 1st to 4th mode shapes of the rectangular plate.

Method	Ω_1	Ω_2	Ω_3	Ω_4
MATLAB Code	1.355	3.1506	4.065	6.6.13
ANSYS software	1.357	3.159	4.076	6.635
LSFD method [8]	1.356	3.303	3.733	6.827

Table 2. Maximum value of the generalized displacement functions for the 1st to 4th modes of the rectangular plate.

	Method	1st Mode	2nd Mode	3rd Mode	4th Mode
w	MATLAB	0.036452	0.044939	0.04029	0.051884
	ANSYS	0.036494	0.045174	0.04042	0.052141
	% Error	0.115	0.52	0.32	0.493
ψ_x	MATLAB	0.042879	-0.029977	0.0828	0.054614
	ANSYS	0.042895	-0.029832	0.08295	0.054309
	% Error	0.0373	-0.45	0.181	0.558
ψ_y	MALTAB	0.0050769	-0.09035	-0.01392	-0.093806
	ANSYS	0.0051129	-0.09077	-0.01396	-0.094166
	% Error	0.704	0.463	0.286	0.382

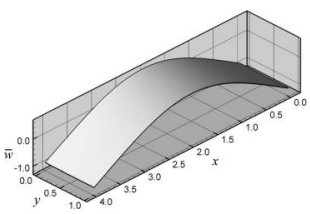

Figure 1. 1st Mode by LSFD

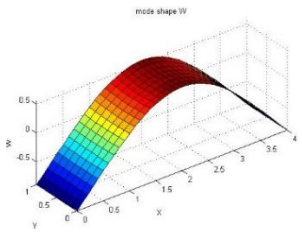

Figure 2. 1st Mode by Ansys

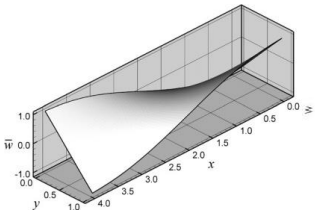

Figure 3. 2nd Mode by LSFD

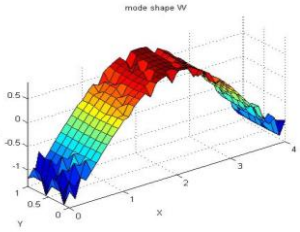

Figure 4. 1st Mode by Matlab

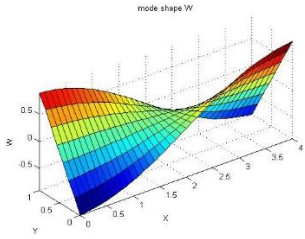

Figure 5. 2nd Mode by Ansys

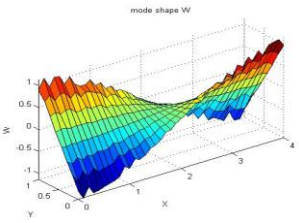

Figure 6. 2nd Mode by Matlab

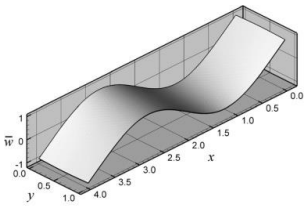

Figure 7. 3rd Mode by LSFD

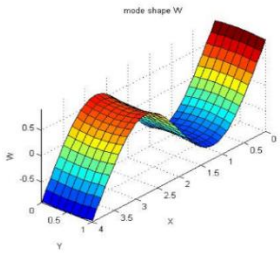

Figure 8. 3rd Mode by Ansys

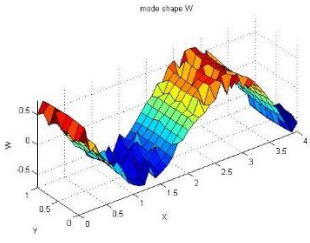

Figure 9. 3rd Mode by Matlab

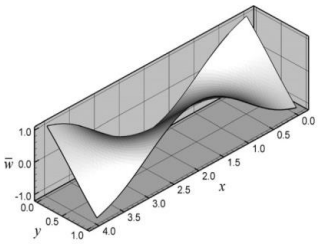

Figure 10. 4th mode by LSFD

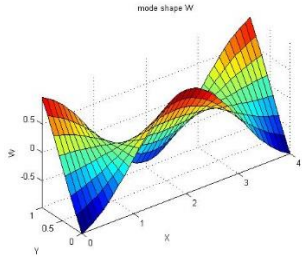

Figure 11. 4th mode by Ansys

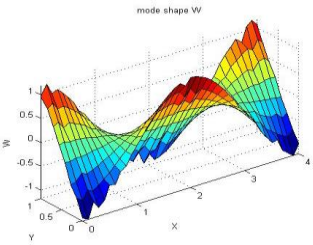

Figure 12. 4th mode by Matlab

3.2. The stress resultants of the rectangular plate

In Table. 3, the maximum values of the stress resultants corresponding to the 1st to 4th mode shapes of the rectangular plate are given. The results are obtained from the MATLAB code, ANSYS software, and LSFD method [8]. Also, figures 13-21 show $\bar{M}_{xx}$, $\bar{M}_{xy}$, and $\bar{Q}_x$ stress resultants associated with the 1st mode, and Figs. 22-27 show $\bar{M}_{yy}$ and $\bar{Q}_y$ stress resultants associated with the 2nd mode. As can be seen, in all three methods, the maximum value of the stress resultants are close enough. However the results of finite element code show some oscillations near free edges as reported in previous research [6].

3.3. The effect of thickness

In order to assess the effect of thickness on the natural frequencies of the rectangular plate, a similar plate with a thickness that is 10% of the original thickness is considered. This plate is modeled by the finite element MATLAB code and the ANSYS software. According to [27] a pontoon-type VLFS can be from few hundred to 5000 meters in length with a depth of 2 to 10 meters. This means a typical VLFS has a depth to length ration greater than 2×10^{-3}. Our numerical model with 4 m length and two thicknesses of 0.1 and 0.01 m have 25×10^{-3} and 2.5×10^{-3} depth to length ratios which are in the acceptable range. For this model, the natural frequencies and frequency parameters are given in Tables 4 and 5, respectively. The two FEM outputs (MATLAB and ANSYS) and the results of LSFD method [8] are compared with each other.

A comparison of values in Tables 1 and 5 shows that for corresponding mode shapes, by increasing the plate thickness the frequency parameter does not change significantly.

In addition, since the frequency parameter Ω in Eq. (19) is proportional with the ratio of natural frequency to thickness, ω/h, its variation for the same thickness is the same as that of ω.

Table 3. Maximum value of the stress resultants for the 1st to 4th modes of the rectangular plate.

Stresses resultants	Method	1st mode	2nd mode	3rd mode	4th mode`
$\bar{M}_x$	MATLAB	1.1021	0.4276	2.985	1.96
	ANSYS	0.9768	0.3367	2.485	1.576
	LSFD[8]	1.016	0.382	2.676	1.717
$\bar{M}_y$	MATLAB	0.0723	0.1901	0.323	0.588
	ANSYS	0.0505	0.1398	0.268	0.502
	LSFD[8]	0.0575	0.145	0.28	0.535
$\bar{M}_{xy}$	MATLAB	0.0474	1.2781	0.401	2.014
	ANSYS	0.045	0.9781	0.288	1.756
	LSFD[8]	0.0499	1.066	0.302	1.942
$\bar{Q}_x$	MATLAB	2.832	43.2382	21.15	73.201
	ANSYS	3.0863	36.2382	18.33	71.498
	LSFD[8]	3.15	38.043	19.126	72.137
$\bar{Q}_y$	MATLAB	0.1368	12.04	0.7126	44.018
	ANSYS	0.1001	10.6515	0.5166	39.797
	LSFD[8]	0.118	11.063	0.593	41.516

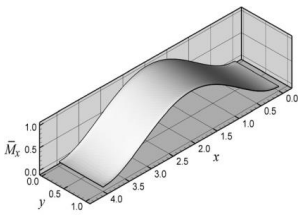

Figure 13. Bending moment $\bar{M}_x$ for 1st mode by LSFD [8]

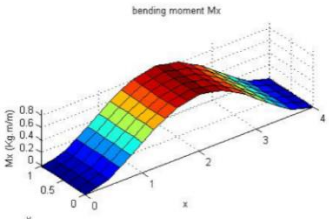

Figure 14. Bending moment $\bar{M}_x$ for 1st mode by ANSYS

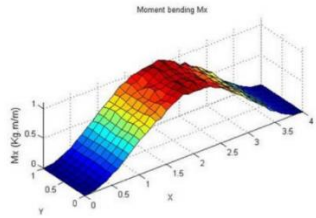

Figure 15. Bending moment for 1st mode by MATLAB

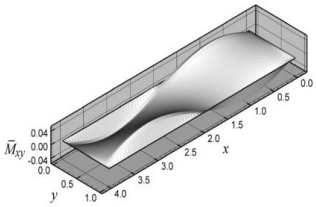

Figure 16. Twisting moment $\bar{M}_x$ $\bar{M}_{xy}$ for 1st mode by LSFD [8]

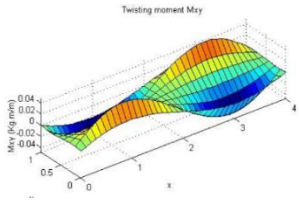

Figure 17. Twisting moment $\bar{M}_{xy}$ for 1st mode by ANSYS

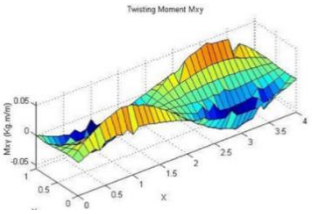

Figure 18. Twisting moment $\bar{M}_{xy}$ for 1st mode by MATLAB.

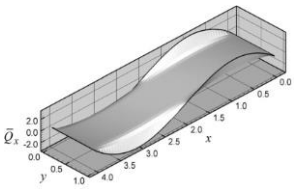

Figure 19.Shear force $\bar{Q}_x$ for 1st mode by LSFD [8]

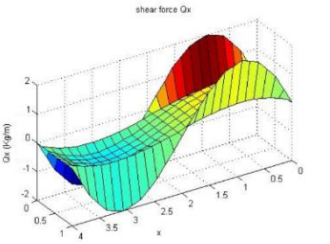

Figure 20. Shear force $\bar{Q}_x$ for 1st mode by ANSYS.

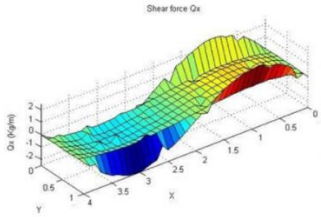

Figure 21.Shear force $\bar{Q}_x$ for 1st mode by MATLAB

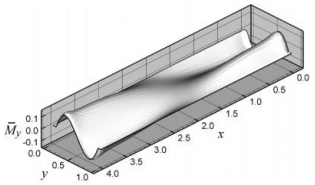

Figure 22. Bending moment $\bar{M}_y$ for 2nd mode by LSFD [8]

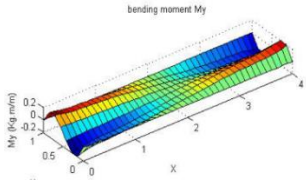

Figure 23. Bending moment $\bar{M}_y$ for 2nd mode by ANSYS

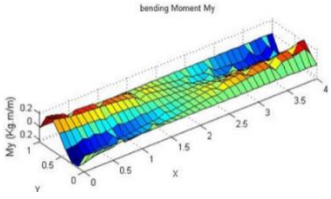

Figure 24. Bending moment $\bar{M}_y$ for 2nd mode by MATLAB

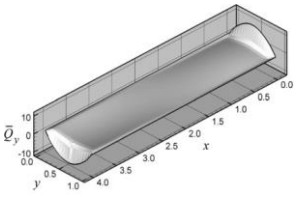

Figure 25. Shear force $\bar{Q}_y$ for 2nd mode by LSFD [8]

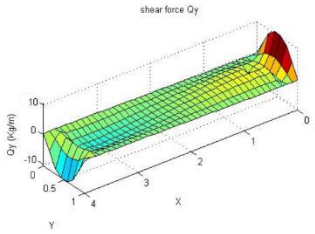

Figure 26. Shear force $\bar{Q}_y$ for 2nd mode by ANSYS.

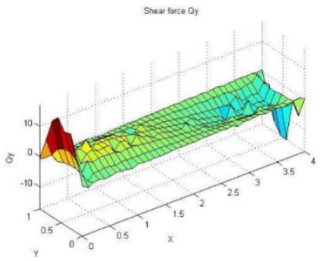

Figure 27. Shear force $\bar{Q}_y$ for 2nd mode by MATLAB

Table. 4. Natural frequencies of the 1st to 4th mode shapes of the rectangular plate with 0.01 m thickness

Method	ω_1	ω_2	ω_3	ω_4
MATLAB	1.0573	2.5724	2.9714	5.3463
ANSYS	1.0568	2.5561	2.9657	5.3080
Error	0.0473	0.634	0.192	0.716

Table. 5. Frequency parameters of the 1st to 4th mode shapes of the rectangular plate with 0.01 m thickness

Method	Ω_1	Ω_2	Ω_3	Ω_4
Matlab	1.3405	3.2614	3.767	6.778
Ansys	1.339	3.2407	3.76	6.729
LSFD[8]	1.338	3.256	3.711	6.751

Table 6. shows the maximum values of the dimensionless stress resultants of the rectangular plate with 0.01 m thickness obtained by FEM (MATLAB and ANSYS) and LSFD [8] methods corresponding to the 1st mode shape. Figs. 28-39 present the distribution of the stress resultants associated with the same mode shape. As can be seen, there are some discrepancies between FEM results and LSFD results at plate free boundaries. This can be due to several reasons. As mentioned before, two major factors are associated with: (1) the presence of steep gradients in stress resultant distributions near free edges, and (2) the weak form of imposing natural boundary conditions at free edges in FEM. It can also be observed that the results of MATLAB code are worse than those of ANSYS. This is because the finite element mesh in MATLAB was rather coarse (140 elements) and the selective reduced integration technique was not implemented.

Table. 6. Maximum value of stress resultants of the 1st mode shape of the rectangular plate with 0.01 m thickness

Method	$\bar{M}_x$	$\bar{M}_y$	$\bar{M}_{xy}$	$\bar{Q}_x$	$\bar{Q}_y$
MATLAB	0.8933	0.0595	0.0552	17.0845	0.2916
ANSYS	0.9121	0.0623	0.0695	17.2976	0.2916
LSFD[8]	1.02	0.0574	0.0676	18.2	0.31

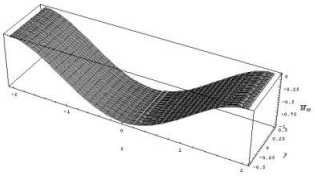

Figure.28. Bending moment $\bar{M}_x$ for 1st mode by LSFD [8]

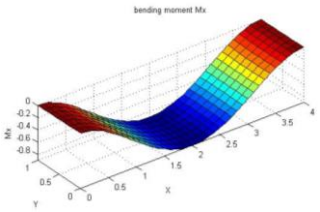

Figure.29. Bending moment $\bar{M}_x$ for 1st mode by ANSYS.

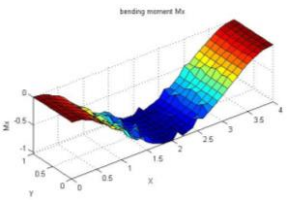

Figure.30. Bending moment $\bar{M}_x$ for 1st mode by MATLAB

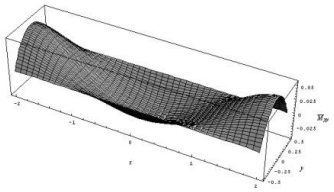

Figure.31. Bending moment $\bar{M}_y$ for 1st mode by LSFD [8]

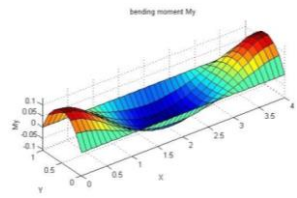

Figure.32. Bending moment $\bar{M}_y$ for 1st mode by ANSYS.

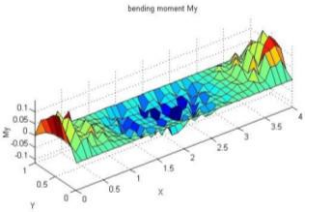

Figure.33. Bending moment $\bar{M}_y$ for 1st mode by MATLAB.

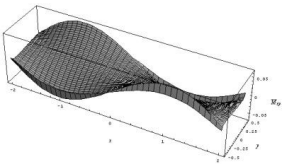

Figure.34. Twisting moment $\bar{M}_{xy}$ for 1st mode by LSFD [8]

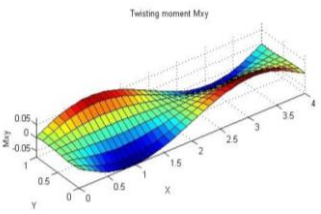

Figure.35. Twisting moment $\bar{M}_{xy}$ for 1st mode by ANSYS.

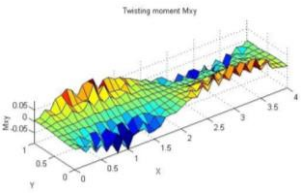

Figure.36. Twisting moment$\bar{M}_{xy}$ for 1st mode by MATLAB.

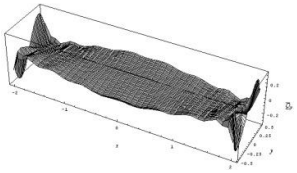

Figure.37. Shear force $\bar{Q}_y$ for 1st mode by LSFD [8]

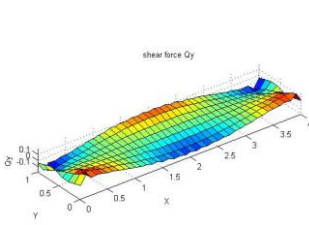

Figure.38. Shear force $\bar{Q}_y$ for 1st mode by ANSYS.

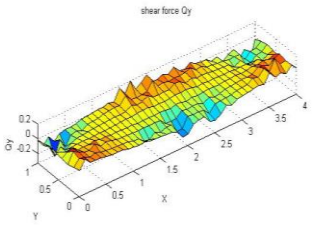

Figure.39. Shear force $\bar{Q}_y$ for 1st mode by MATLAB.

4. Conclusions

An attempt has been made to investigate the dynamic behavior of very large pontoon-type floating structures using finite element method. To this end, the structure has been modelled as a rectangular plate with free edges. A finite element code was written in MATLAB based on the Mindlin plate theory. The same problem was analyzed with ANSYS. Two plates with 0.1m and 0.01m thicknesses are considered. Natural frequencies, mode shapes and stress resultants of rectangular plates were predicted. The effect of thickness on plate's dynamic behavior was studied. It is observed that the increase in plate natural frequencies is proportional with the increase in plate thickness. The FEM results obtained from the MATLAB code and ANSYS software were compared with each other as well as with the results of a least squares finite difference method reported by [8]. It is revealed that the FEM results are satisfactory for natural frequencies and mode shapes, while the finite element results for stress resultants at plate' free edges were not satisfactory. This agrees with similar results reported in the literature.

5. References

1- Watanabe, E., Utsunomiya, T., and Wang, C.M., (2004), *Hydroelastic analysis of pontoon-type VLFS: a literature survey*, Engineering Structures Vol. 26, pp. 245-256.

2- Utsunomiya, T., (2008) *in* Very Large Floating Structures, Edited by Wang, C.M., Watanabe, E., and Utsunomya, T., Taylor & Francis.

3- Liew, K. M., Han, J. B., (1995), *Differential quadrature method for Mindlin plates on Winkler foundations*, International Journal of Mechanical Science. Vol. 38, pp. 405-421.

4- Xiang, Y., (1995), *Vibration analysis of rectangular Mindlin plates resting on elastic edge supports*, *Journal of Sound and Vibration*, Vol. 204, pp. 1-16.

5- Rossi, R. E., and Bambill, D. V., (1997). *Vibrations of a rectangular orthotropic plate with a free edge: A comparison of analytical and numerical results*, Ocean Engineering, Vol. 25, pp. 521–527.

6- Wang, C. M., Xiang, Y., Utsunomiya, T., Watanabe, E., (2000), *Evaluation of modal stress resultants in freely vibrating plates*, International Journal of Solids and Structures, Vol. 38, pp. 6525-6558.

7- Beirao da Veiga, L., (2004), *Finite element methods for a modified Reissner–Mindlin free plate model*, SIAM Journal on numerical analysis Vol. 42, pp. 1572–1591,

8- Wang, C. M., Wu, W. X., Sha, C., Utsanomiya, T., (2006), *LSFD method for accurate vibration modes and modal stress–resultants of freely vibrating plates that model VLFS*, Computers and Structures, Vol. 84, pp. 2329–2339.

9- Wu, W. X., Shu, C., Wang, C. M., (2006), *Computation of modal stress resultants for completely free vibrating plates by LSFD method*, Journal of Sound and Vibration, Vol. 297, pp. 704-726.

10- Ma, Y. Q., Ang, K. K., (2006), *Free vibration of Mindlin plates based on the relative displacement plate element*, Finite Element in Analysis and Design. Vol. 42, pp. 929-1030.

11- Sadrnejad, S. A., Saedi Daryan, A., (2009) *Vibration equation of thick rectangular plates using Mindlin plate theory*, Journal of Computer Science. Vol. 5, pp. 838-842.

12- Xiang, Y., Lai, S.k., and Zhou, L., (2010), *DSC-element method for free vibration analysis of rectangular Mindlin plates*, International Journal of Mechanical Sciences Vol. 52, pp. 548-560.

13- Xiang, Y., Lai, S.k., and Zhou, L., Lim, C.W., (2010), *DSC-Ritz element method for vibration analysis of rectangular Mindlin plates with mixed edge supports* European Journal of Mechanics, Vol. 24, pp. 619-628.

14- Hosseini-Hashemi, Sh., Rokni Damavandi Taher., Akhavan, H., and Omidi, M., (2010), *Free vibration of functionally graded rectangular plates using first-order shear deformation plate theory*, Applied Mathematical Modelling Vol. 34, pp. 1276-1261.

15- Hosseini-Hashemi, Sh., Fadaee, M., and Atashipour, S.R., (2011), *A new exact analytical approach for free vibration of Reissner-Mindlin Functionally graded rectangular plates*. International Journal of Mechanical Sciences Vol. 53, pp. 11-22.

16- Hosseini-Hashemi, Sh., Fadaee, M., and Rokni Damavandi Taher, H., (2011), *Exact solution for free flexural vibration of Levy–type rectangular thick plates via third-order shear deformation plate theory*. Applied Mathematical Modelling Vol. 35, pp. 708-727.

17- Ramu, I., and Mohanty, S.C., (2012). *Study on free vibration analysis of rectangular plate structures using finite element method,* Procedia Engineering Vol. 38, pp. 2758-2766.

18- Pereira, W.l.a., Karam, V.J., Carrer, J.A.M., and Mansur, W.J., (2012), *A dynamic formulation for the analysis of thick elastic plates by the boundary element method*. Engineering Analysis with Boundary Elements, Vol. 36, pp.1138–1150.

19- Eftekhari, S.A., and Jafari, A.A., (2013). *Modified mixed Ritz-DQ formulation for free vibration of thick rectangular and skew plates with general boundary conditions*, Applied Mathematical Modelling Vol. 37, pp. 7398-7426.

20- Cho, D.S., Vladimir, N., and Choi, T.M., (2013), *Approximate natural vibration analysis of rectangular plates with opening using assumed mode method*. Int. J. Naval Archit. Ocean Eng. Vol. 5, pp. 478-491.

21- Thai, H.T., and Choi, D.H., (2013), *Analytical solutions of refined plate theory for bending bucking and vibration analyses of thick plates*, Applied Mathematical Modelling Vol. 37, pp. 8310-8323.

22- Senjanovic, I., Vladimir, N., and Hadzic, N., (2015), *Modified Mindlin plate theory and shear locking–free finite element formulation*, Mechanics Research Communication Vol. 55, pp. 95-104.

23- Praveen, K.M., Karmakar, D., and Nasar, T., (2016), *Hydroelastic analysis of floating elastic thick plate in shallow water depth*, Perspectives in Science Vol. 8, pp. 770-772.

24- Senjanovic, I., Tomic, M., Hadzic, N., and Vladimir, N., (2017), *Dynamic finite element formulations for moderately thick plate vibtations based on the modified Mindlin theory*, Engineering Structures Vol. 139, pp. 100-113.

25- Khezri, M., Gharib, M., and Rasmusse, K.J.R., (2018), *A unified approach to meshless analysis of thin to moderately thick plates based on a shear-locking-free Mindlin theory formulation*, Thin-Walled Structures Vol. 124, pp. 161-179.

26- Shirkol, A.I., and Nasar, T., (2018), *Coupled boundary element method and finite element method for hydroelastic analysis of floating plate*. Journal of Ocean Engineering and Science Vol. 3, pp.19-37.

27- Wikipedia, (2018), Very Large Floating Structures, http://en.wikipedia.org/wiki/very_large_floating_structures. August 7, 2018.